Supplementary Information

MATERIALS AND METHODS

Cell culture

T6PN cell cultures[1] were infected with retrovirus expressing hTERT.[2] After 3 passages, the cell culture was further infected with VSV-G pseudotyped retrovirus expressing E47 as a fusion protein with the modified estrogen receptor (E47mer; kind gift from Kees Murre).[3] The vector also contained the CD25 cell surface marker, permitting the use of fluorescence-activated cell sorting (FACS) to sort infected cells. The cell line expressing telomerase and E47 was termed T6PNE. It was maintained in Dulbecco's modified Eagle's medium (DMEM) and 5.5 mM glucose supplemented with 10% fetal bovine serum (FBS). To induce E47 activity in cells under experimental conditions, we added tamoxifen (0.5-10 µM) to the culture media. BrdU incorporation studies were performed with BrdU (GE, Piscataway, NJ) added to cells for up to 2 h. For structure-activity relationship (SAR) studies, compounds were added to cells for 48 h. For chronic ethopropazine treatment, T6PNE cells were seeded in 0.5 µM tamoxifen. At 24 h, either 15 µM ethopropazine or a vehicle control was added. At 96 h, the cells were passed into either a 384-well clear-bottom black well plate for imaging or to a culture dish with fresh ethopropazine or vehicle. The same passing procedure was performed every 3 days for the remainder of the 12-day experiment ($n = 3$; experiment was performed 3 times; error bars are standard error; $p < 0.05$). HeLa cells were maintained in DMEM (GIBCO, Carlsbad, CA) and 10% FBS. Human islets were obtained from the NIH/JDRF Islet Cell Resource Center Program.

Vector design and transfection studies. HeLa cells (ATCC, Manassas, VA) were transfected by the $CaPO_4$ method with full-length Kip2 promoter or Kip2 promoter deletion constructs provided by Dr. S. Okret (Huddinge University Hospital, Sweden).[4] To analyze E-box activity, HeLa cells were transfected with (4RTK-luc)[5] reporter and a plasmid encoding either wtE47 or E47mer.[3] Sixteen hours after transfection, the culture medium was changed and maintained for 48 h with or without tamoxifen.

Human Kip2 cDNA was cloned from pBlueskriptR (Open Biosystems, Huntsville, AL) into the MSCV-IRES-GFP vector.[6] Lentivirus expressing the insulin promoter driving green fluorescent protein (GFP) was produced as previously described.[7] For lentivirus expressing shKip2, 4 different siRNA target sequences were chosen from the open reading frame of human Kip2 (accession no. BC067842), using the siRNA selection algorithm from sfold (http://sfold.wadsworth.org/).

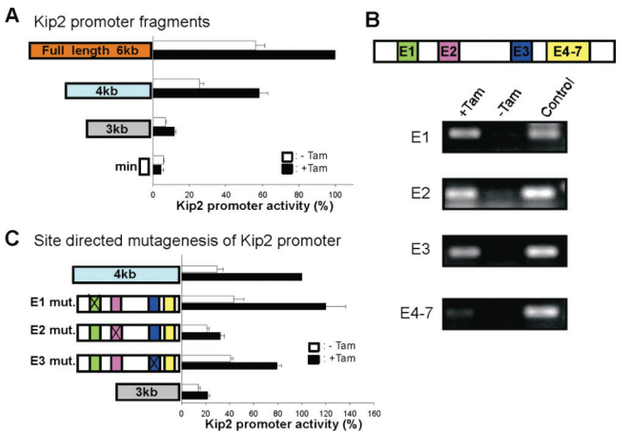

FIG. S1. Kip2 promoter responsiveness to E47. (**A**) A 6.3-kb and several shorter fragments from the 5′ region of the Kip2 gene were cloned upstream of a luciferase reporter gene and luciferase activity measured in the absence and presence of 4 µM tamoxifen, with the finding that the region responsive to E47 was localized to a 900-bp fragment between 3 and 4 kb 5′ of the transcription start site. (**B**) This region was found to contain 7 E-box elements in 4 distinct locations, with E4-E7 clustered together. ChIP analysis revealed weak binding to the E4-E7 cluster and strong binding to E1-3. (**C**) Site-directed mutagenesis of E1 (green), E2 (magenta), and E3 (blue) demonstrated that only E2 was required for E47-responsiveness.

An H1 promoter-driven shRNA expression cassette was constructed by amplification of an oligonucleotide containing the entire shRNA, as described.[8] Each shRNA cassette was digested with XbaI and ligated into pBluescript. Validation of the construct was done by cotransfection with a plasmid expressing Kip2. The most effective shRNA cassette, as determined by Western blot, was transferred into a lentiviral vector for virus production.[8,9]

For Kip2 oligonucleotides, the start position is shown of the siRNA target sequence and the sequence of the oligonucleotide used for amplification: (shKip2-1448) 5′-CTGTCTAGACA AAAACCAAGGTGTAAAGCTTTAATCTCTTGAATTAA AGCTTTACACCTTGGGG GGATCTGTGGTCTCATACA.

RT-PCR. Quantitative RT-PCR was performed on cDNA corresponding to 100 ng of RNA using the Opticon Real-Time

Journal of Biomolecular Screening XX(X); XXXX
DOI: 10.1177/1087057110372257

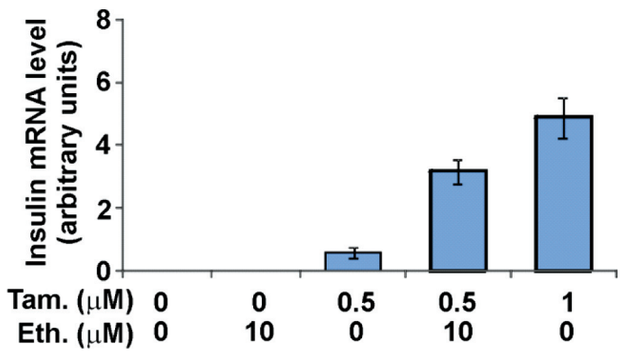

FIG. S2. Phenothiazines do not exhibit estrogenic behavior. T6PNE cells were exposed to tamoxifen (Tam.) for 3 days and/or ethopropazine (Eth.) for the final 48 h, followed by extraction of RNA and quantitative real-time RT-PCR for insulin and GAPDH. Insulin mRNA was normalized to GAPDH, which did not vary significantly between the samples. In the absence of tamoxifen, insulin mRNA was not induced by ethopropazine, demonstrating that ethopropazine did not exhibit activation of the $E47^{MER}$ fusion protein in a manner similar to tamoxifen. Error bars are SD of 3 biological replicates.

System (MJ Research, Waltham, MA) with SYBR Green. RT-PCR for GAPDH was used for normalization. To measure the number of copies of mRNA, standard curves were constructed by PCR with a known number of copies of the target sequence.

Primers:

Glucokinase for: gaagggaatgcttgccgactcgttgg; rev: cacactggcctcttcatgggtctc

SUR-1 for: cctcgatgccatcatcacagaa; rev: cagcttctctggcttatcgaac

Insulin, MafA, and GAPDH primers were described previously.[10]

Western blot. Whole-cell extracts were prepared by incubation in RIPA buffer containing protease inhibitors (Calbiochem, San Diego, CA). Protein (20 μg) was separated on 4% to 20% Longlife gels (LifeGels, Newcastle upon Tyne, UK) and transferred to Immobilon-P membrane (Millipore, Billerica, MA). After overnight blocking in phosphate-buffered saline–Tween (PBST) with 3% milk, membrane was incubated with Kip2 antibody (Santa Cruz Biotechnology, Santa Cruz, CA), followed by secondary antibody conjugated to horseradish peroxidase (Amersham/GE, Buckinghamshire, UK) and signal revealed by ECL (Amersham/GE).

ChIP assay. T6PNE cells treated with or without 10 μm tamoxifen were treated with formaldehyde for in vivo cross-linking of Kip2 promoter and E47. Cross-linking was quenched by addition of glycine. The cells were then harvested by centrifugation resuspended in lysis buffer, according to the EZ-ChIP protocol (Upstate, Billerica, MA).

Cellular DNA was sheared by sonication and immunoprecipitated with E47 antibody (Santa Cruz Biotechnology). Following purification, PCR was used to analyze immunoprecipitated DNA. PCR of 10 ng DNA was performed with E-box oligonucleotide primers from the region between 4 kb and 3 kb in Kip2 promoter deletion constructs. PCR products were analyzed by electrophoresis on 1.2% agarose gels.

First:

F: 5′ GGGGCGTTACATACCCTAA
R: 5′ CCACCAACCCAGCTAATTT

Second:

F: 5′ AAGCCTGGGCAACATAGAGA
R: 5′ TAGAGGGCGTCTTGCTCTGT

Third:

F: 5′ CAATCCTGGTGGATCTTCGT
R: 5′ CAGTGTGTTTGCTCTGGAA

Fourth to sixth:

F: 5′ TTCCAGAGGCAAACACACTG
R: 5′ CATTCCTAGCCCTGTGAAGC

Mutagenesis study. The 4-kb Kip2 deletion construct was used to make point mutations in each E-box between 4 kb and 3 kb by the QuikChange II XL Site-Directed Mutagenesis kit (Stratagene, La Jolla, CA).

The PCR-based protocols were allowed to proceed for 18 cycles with each E-box point-mutated primers. The product was treated with Dpn I restriction enzyme at 37 °C for 1 h to digest the parental DNA template and to select for mutation containing synthesized DNA. The mutated DNA was transformed in XL10-Gold Ultracompetent cells and purified with Endo-free Plasmid Maxi kit (QIAGEN, Valencia, CA).

Kip2 promoter (Sac4.0) first E-box mutation primer:

5′-GGAGACCAAGGCCGGGCTCGCTTG-3′
5′-CAAGCGAGCCCGGCCTTGGTCTCC-3′

Kip2 promoter (Sac4.0) second E-box mutation primer:

5′-GGTGTGGTGGAATTCCTGTGGTCC-3′
5′-CCACACCACCTTAAGGACACCAGG-3′

Kip2 promoter (Sac4.0) third E-box mutation primer:

5′-TCGTTAAGCCCGGTTTCCCAGGGG-3′
5′-CCCCTGGGAAACCGGGCTTAACGA-3′

Luciferase and CAT assays. Cells transfected with Kip2 promoter constructs driving a luciferase reporter gene as well as CMV-CAT were harvested with lysis buffer. Kip2 promoter activity was measured by the Luciferase Reporter Gene Assay kit (Roche, Basel, Switzerland), and data were normalized to CAT activity (Roche).[1]

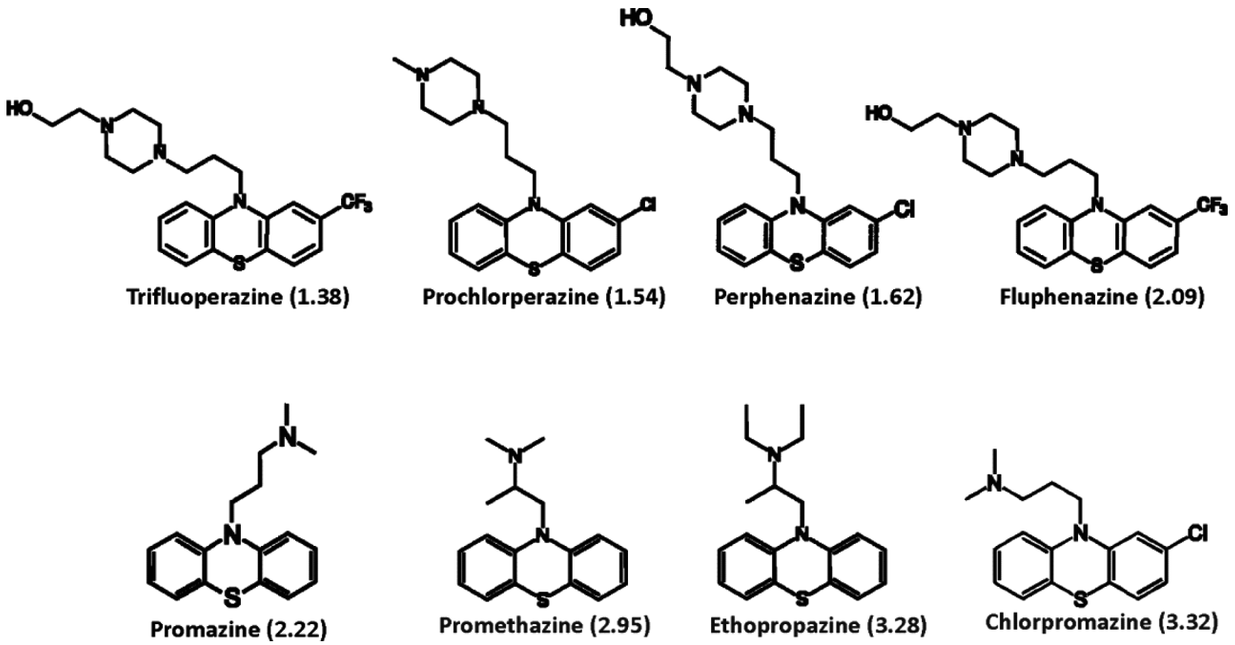

FIG. S3. Structure-activity relationship of phenothiazine compounds from the NIH/JDRF library. Numbers in parentheses are the fold change in green fluorescent protein (GFP) fluorescence in T6PNE cells induced by that compound (taken from **Fig. 5B**).

Immunohistochemistry. Immunostaining was performed on monolayers fixed with 4% paraformaldehyde and blocked with 5% donkey serum (Jackson ImmunoResearch Laboratories, West Grove, PA) and 1% bovine serum albumin (Sigma, St. Louis, MO) in PBS. Primary antibodies were mouse monoclonal anti-E47 (Santa Cruz Biotechnology), mouse anti-Kip2 (Diagnostic BioSystems, Pleasanton, CA), and mouse anti-BrdU (GE). Secondary antibodies were Rhodamine red donkey anti-mouse (Jackson ImmunoResearch Laboratories) and fluorophore-labeled donkey anti-mouse (Alexa Fluor 488, Molecular Probes, Eugene, OR). Samples were mounted in Vectashield (Vector Labs, Burlingame, CA). Digital images of stained sections were captured using a fluorescence microscope with a digital camera (Nikon, Tokyo, Japan).

Arrays and analysis. Microarray analysis was used to determine genes expressed in T6PNE cells. RNA isolated from T6PNE cells treated with and without tamoxifen was assayed for the expression of 24,000 human genes using Illumina BeadArray microarrays and Bead Studio software. Microarray data have been submitted in MIAME-compliant format to the Gene Expression Omnibus (GEO) database (GSE18821).

High-throughput screening

Compound library screening. T6PNE cells expressing the insulin-eGFP transgene were plated at 2000 cells per well in a 384-well plate in the presence of 0.5 μM tamoxifen to induce a submaximal level of insulin expression. That dose of tamoxifen was chosen to allow the screen to be particularly sensitive to compounds that upregulated insulin promoter activity. A higher dose of tamoxifen would be optimal to detect compounds that inhibited the insulin promoter. Compound addition was performed 24 h after tamoxifen administration with the BiomekFX (Beckman Coulter, Fullerton, CA). This was done by adding a single compound from the NIH/JDRF Custom Collection compound library (MicroSource Discovery Systems, Gaylordsville, CT). All compounds were to a final concentration in the well of 5 μM. Forty-eight hours after compound addition, the cells were fixed in 4% paraformaldehyde and stained with DAPI (0.167 μg/mL) to allow DNA content on a per cell basis (a surrogate for cell number) to be measured. The plates were stored in 50% glycerol.

Image acquisition and analysis. Images were obtained on a Beckman Coulter IC 100 high-throughput microscopy system equipped with a Hamamatsu ORCA-ER scientific camera using a Nikon S Flour 10 × NA 0.5 objective. Each 384-well plate was scanned and DAPI (40 ms integration time), GFP (200 ms integration time), and RFP channels were collected at one 3-color, 1280 × 1024 image per well.

Images of each well were captured in the blue channel to evaluate DAPI fluorescence as a measure of cell number, the green channel to assess expression of the insulin promoter–GFP

Table S1. Islet-Enriched Genes Expressed in T6PNE Cells Treated with Tamoxifen

GI_5032100-S	ABCC5	MRP5; SMRP; ABC33; MOATC; MOAT-C; pABC11; EST277145
GI_11545766-S	ABHD4	FLJ12816
GI_21327681-S	ACADM	MCAD; ACAD1; MCADH
GI_4557232-S	ACADS	SCAD; ACAD3
GI_7710156-A	ACHE	YT
GI_13325060-S	ACTR1B	ARP1B; CTRN2
GI_10862690-S	ACVR1	ALK2; SKR1; ACTRI; ACVRLK2
GI_7662201-S	ADAMTSL2	
GI_4501944-S	ADM	AM
GI_6138971-S	ADRBK1	GRK2; BARK1; BETA-ARK1
GI_26787963-A	AGPAT1	G15; LPAATA; MGC4007; MGC5423; 1-AGPAT1; LPAAT-alpha
GI_6041664-S	AGPAT2	BSCL; BSCL1; LPAAB; LPAAT-beta
GI_4501992-S	AGPS	ADAS; ADPS; ADAP-S; ADHAPS; ALDHPSY
GI_24469782-S	AGTRAP	ATRAP
GI_41107701-S	AHDC1	
GI_4502010-S	AK1	
GI_7657354-S	AKAP8L	
GI_24497580-S	AKR1C1	C9; DD1; DDH; DDH1; H-37; MBAB; HAKRC; MGC8954; 2-ALPHA-HSD; 20-ALPHA-HSD
GI_24497581-S	AKR1C2	DD; DD2; BABP; DDH2; HBAB; HAKRD; MCDR2; AKR1C-pseudo
GI_4885060-S	AKT1	PKB; RAC; PRKBA; RAC-ALPHA
GI_34577109-A	ALDOA	ALDA; MGC10942; MGC17716; MGC17767
GI_31541901-S	AMBP	HCP; ITI; UTI; ITIL
GI_21071002-A	AMFR	GP78; RNF45
GI_4502094-S	ANPEP	CD13; LAP1; PEPN; gp150
GI_9625245-S	ANXA10	ANX14
GI_22027652-A	AP1B1	ADTB1; BAM22; AP105A; CLAPB2
GI_16950626-A	AP1S1	AP19; CLAPS1; SIGMA1A
GI_19913415-A	AP2A1	ADTAA; CLAPA1; AP2-ALPHA
GI_11038642-A	AP2S1	AP17; CLAPS2; AP17-DELTA
GI_7705786-S	APH-1A	APH1A; CGI-78
GI_6995997-S	ARF1	
GI_28416434-A	ARFGAP1	ARF1GAP; MGC39924; HRIHFB2281
GI_28416437-S	ARFGAP3	ARFGAP1
GI_33466360-S	ARFRP1	ARP
GI_34147601-S	ARHGDIA	GDIA1; RHOGDI
GI_15011971-S	ARHGEF1	GEF1; LBCL2; SUB1.5; P115-RHOGEF
GI_15011976-S	ARHGEF16	NBR; GEF16
GI_8923906-A	ARL6IP4	SR-25; SRp25
GI_20127415-S	ARNTL	TIC; JAP3; MOP3; BMAL1; MGC47515
GI_22748652-S	ARRDC1	
GI_18373304-S	ARRDC2	
GI_4502246-S	ARVCF	
GI_30089993-A	ASB7	FLJ22551
GI_9966896-S	ATP13A1	
GI_28373114-A	ATP2A3	SERCA3
GI_34335257-S	ATP6V0D1	P39; VATX; Vma6; ATP6D; ATP6DV; VPATPD
GI_22538424-S	ATPAF2	ATP12; ATP12p; MGC29736
GI_15451880-A	B3GALT5	B3T5; GLCT5; B3GalTx; B3GalT-V; beta3Gal-T5
GI_12408653-S	B3GAT3	GLCATI; GlcAT-I
GI_14670387-A	BAD	BBC2; BCL2L8
GI_5453564-A	BAIAP2	BAP2; IRSP53
GI_15451913-S	BAIAP3	BAP3; KIAA0734
GI_5031608-S	BCKDK	
GI_20336474-A	BCL7B	
GI_32698935-S	BCL9L	DLNB11
GI_21536418-S	BIK	BP4; NBK; BBC1; BIP1
GI_21536416-A	BIN1	AMPH2; AMPHL; SH3P9; MGC10367; DKFZp547F068
GI_20127587-S	BIN3	
GI_13123777-S	BRUNOL4	CELF4; BRUNOL-4
GI_20127579-S	BTBD2	FLJ20386
GI_28872718-S	BTG2	PC3; TIS21

(continued)

Table S1. (continued)

GI_37551029-S	C100rf38	
GI_7019334-S	C110rf9	KIAA0954; MGC10781
GI_13124889-S	C120rf8	ERP28; ERP29; ERp31; PDI-DB
GI_18491027-S	C150rf15	L30; RLP24; RPL24; RPL24L; HRP-L30-iso
GI_27734946-S	C150rf26	
GI_21700762-S	C160rf34	HN1L; FLJ13092
GI_4757805-S	C160rf7	ATP-BL
GI_37552310-S	C190rf20	
GI_34098936-S	C190rf6	ASBABP1; MGC4022; R32184_3
GI_27363487-S	C1QG	C1QC
GI_34222385-S	C1QL1	
GI_32967299-A	C1QTNF6	CTRP6; ZACRP6
GI_34147371-S	C200rf149	MGC2479; FLJ21046; dJ697K14.9
GI_31542254-S	C200rf160	dJ310013.5
GI_23510349-A	C200rf161	SNX-L; SNX21; PP3993; MGC29895; dJ337018.4
GI_31341351-S	C200rf178	Shax1; CHMP4A; CHMP4B; dJ553F4.4
GI_8923517-S	C200rf27	FLJ20550
GI_34147345-S	C200rf67	PCIF1
GI_20127520-S	C220rf5	HS506A; DKFZP586A1024
GI_31542710-S	C20rf18	
GI_20070263-S	C20rf30	
GI_24308070-S	C20rf32	
GI_27544938-S	C30rf10	
GI_20149669-S	C60rf106	
GI_8393383-S	C60rf48	G8; D6S57
GI_27478738-S	C90rf150	MGC46502
GI_34147359-S	C90rf16	MGC4639; EST00098; FLJ12823
GI_27734964-S	C90rf75	
GI_9951925-S	CA4	CAIV
GI_34147521-S	CABC1	
GI_32698883-S	CABP7	MGC57793
GI_27597079-S	CACNA1C	CaV1.2; CCHL1A1; CACNL1A1
GI_26051217-A	CAMK2B	CAM2; CAMK2; CAMKB; MGC29528
GI_26667190-A	CAMK2G	CAMK; CAMKG; CAMK-II; MGC26678
GI_12408655-S	CAPN1	CANP; muCL; CANPL1; muCANP
GI_37577156-S	CAPN5	HTRA3; nCL-3
GI_19923793-S	CARD10	BIMP1; CARMA3
GI_10190681-S	CBX8	PC3; RC1; HPC3
GI_4759075-S	CCL20	CKb4; LARC; ST38; MIP3A; MIP-3a; SCYA20
GI_34147397-S	CCM2	
GI_34328914-A	CD151	GP27; SFA1; PETA-3
GI_5174408-S	CD2BP2	
GI_21237760-S	CD81	S5.7; TAPA1
GI_34147599-S	CD99	MIC2; MIC2X; MIC2Y
GI_16357476-S	CDC34	UBE2R1; E2-CDC34
GI_34452716-A	CDC42EP1	CEP1; BORG5; MSE55; MGC15316
GI_30089963-S	CDC42EP2	CEP2; BORG1
GI_32528264-A	CDK10	PISSLRE
GI_4557440-S	CDKN1C	BWS; WBS; p57; BWCR; KIP2
GI_16945965-S	CENTB5	KIAA1716
GI_21264595-A	CENTD2	ARAP1; KIAA0782
GI_8922520-S	Cep72	
GI_16905523-S	CES1	CEH; CES2; HMSE; SES1; HMSE1
GI_6995995-S	CFTR	CF; MRP7; ABC35; ABCC7
GI_7706275-A	CGI-38	
GI_10800418-S	CHGA	CGA
GI_34222219-S	CHPF	CSS2; FLJ22678
GI_9951921-S	CIB1	CIB; KIP; SIP2-28; CALMYRIN
GI_4502848-S	CKAP1	CG22; TBCB; CKAPI
GI_5803001-S	CLCN2	CLC2; ECA3; EGI3; EGMA; CIC-2
GI_20070131-S	CLCN7	CLC7; CLC-7; OPTA2

(continued)

Table S1. (continued)

GI_5174418-S	CLPP	
GI_4502896-S	CLPTM1	
GI_32483393-A	CLTB	LCB
GI_4502904-S	CLU	CLI; APOJ; SGP2; SGP-2; SP-40; TRPM2; TRPM-2; MGC24903
GI_29789254-A	CMIP	KIAA1694
GI_7657386-S	CNOT3	NOT3; LENG2; NOT3H; KIAA0691
GI_22095394-S	COASY	
GI_17738300-S	COL7A1	EBD1; EBR1; EBDCT
Systematic	Common	Synonyms
GI_6466449-A	COMT	
GI_7705806-S	COQ4	CGI-92
GI_14149733-S	COR01B	CORONIN-2; DKFZP762I166
GI_14249581-S	COR06	
GI_38327637-S	CREB3	LZIP; LUMAN; MGC15333; MGC19782
GI_16418354-S	CREB3L1	
GI_22095396-S	CRELD1	AVSD2; CIRRIN; DKFZP566D213
GI_21361081-S	CRLF1	NR6; CISS; CLF-1
GI_21359983-S	CSDA	DBPA; ZONAB
GI_42658675-S	CSGlcA-T	
GI_21314777-S	CSNK1G2	CK1g2
GI_4503126-S	CTNNA1	CAP102
GI_22749312-S	CUZD1	
GI_4506850-S	CXCL6	GCP2; CKA-3; GCP-2; SCYB6
GI_4557504-S	CYBA	
GI_23957705-S	CYBASC3	
GI_19923602-S	CYBRD1	DCYTB; FLJ23462
GI_38454323-S	CYGB	HGB; STAP
GI_34222286-S	CYR61	CCN1; GIG1; IGFBP10
GI_4557510-S	DAPK3	ZIP; ZIPK
GI_13259507-A	DCTN1	P135; DP-150; DAP-150
GI_34335254-S	DCTN2	RBP50; DCTN50; DYNAMITIN
GI_34147657-S	DDIT3	CHOP; CEBPZ; CHOP10; GADD153
GI_38327631-A	DDR1	CAK; DDR; NEP; PTK3; RTK6; TRKE; CD167; EDDR1; MCK10; NTRK4; PTK3A
GI_19743936-S	DDX27	RHLP; Rrp3p; PP3241; HSPC259; MGC1018; FLJ12917; FLJ20596; FLJ22238; dJ686N3.1; DKFZp667N057
GI_34222345-S	DDX49	FLJ10432; R27090_2
GI_19923594-S	DDX54	DP97; APR-5; MGC2835
GI_14670395-A	DEDD	DEFT; KE05; DEDD1; FLDED1; CASP8IP1
GI_20537349-S	DFNB31	
GI_7382489-S	DGAT1	DGAT; ARGP1
GI_13027629-S	DGCR14	ES2; DGSI; DGS-I; Ese2el
GI_4826693-S	DGCR2	IDD; LAN; DGS-C; SEZ-12; KIAA0163
GI_15718677-S	DGCR6L	FLJ10666
GI_31742531-S	DIAPH1	DRF1; DFNA1; LFHL1; hDIA1
GI_34335250-A	DLGAP4	
GI_5031770-S	DNAJC4	HSPF2; MCG18; DANJC4
GI_4826699-S	DNM2	DYNII
GI_40217610-S	DOCK6	KIAA1395
GI_20070301-S	DOK4	FLJ10488
GI_29544739-A	DOK5	MGC16926; C200rf180
GI_4758189-S	DPEP1	MDP; RDP
GI_24430133-I	DPM3	MGC34275
GI_18426972-S	DRAP1	NC2-alpha
GI_9257200-S	DRD1IP	
GI_24308252-S	DTX2	RNF58; KIAA1528
GI_28872752-S	DUOX2	LNOX2; THOX2; NOXEF2; P138-TOX
GI_4758215-S	DVL2	
GI_12669914-S	E2F4	E2F-4
GI_12669916-S	E2F5	E2F-5
GI_4503446-S	ECH1	HPXEL
GI_12707569-S	ECHS1	SCEH
GI_25453470-S	EEF1A2	HS1; STN; EF1A; EEF1AL; EF-1-alpha-2

(continued)

Table S1. (continued)

GI_25453476-S	EEF2	EF2; EEF-2
GI_37059736-S	EFHD2	
GI_33359679-A	EFNA1	B61; EFL1; ECKLG; EPLG1; LERK1; TNFAIP4
GI_20127546-S	EGFL7	ZNEU1
GI_18141577-A	EGLN2	EIT6; PHD1; HIFPH1; DKFZp434E026
GI_4503516-S	EIF3S4	EIF3-P42; eIF3-p44; eIF3-delta
GI_38201618-A	EIF4G1	p220; EIF4G
GI_11496880-S	ELK1	
GI_13489092-S	ELOVL1	Ssc1; CGI-88
GI_19263346-S	EMID2	
GI_14042987-S	EMILIN2	FOAP-10; EMILIN-2; FLJ33200
GI_4503562-S	EMP3	YMP
GI_4557420-S	ENTPD2	CD39L1; NTPDase-2
GI_4557422-S	ENTPD6	CD39L2; IL6ST2; IL-6SAG; NTPDase-6; dJ738P15.3
GI_32967310-S	EPHA2	ECK
GI_7019368-S	EPN1	
GI_24307980-S	EXOSC7	RRP42
GI_32698727-S	FAM20C	DKFZp547D065
GI_4758219-S	FAM50A	9F; XAP5; HXC-26
GI_12232376-S	FANCF	FAF
GI_16933539-S	FAP	FAPA; DPPIV; SEPRASE
GI_14971419-A	FASTK	FAST; FLJ13079
GI_16306579-S	FBXL11	FBL7; CXXC8; FBL11; LILINA; FLJ00115; KIAA1004; DKFZP434M1735
GI_30749197-A	FBXW5	MGC20962; DKFZP434B205
GI_14150057-S	FBXW9	
GI_8923788-S	FEV	FEV; PET-1
GI_13112049-A	FGFR4	TKF; JTK2
GI_17149850-S	FKBP8	FKBP38; FKBPr38
GI_22547155-S	FLII	FLI; FLIL; Fli1; MGC39265
GI_19923809-S	FLJ20254	
GI_8923451-S	FLJ20489	
GI_42662787-S	FLJ39609	
GI_42491369-S	FLJ43806	
GI_4503744-S	FLNA	FLN; FMD; MNS; ABPX; FLN1; NHBP; OPD1; OPD2; ABP-280
GI_4758393-S	FLOT2	ESA; ECS1; ESA1; ECS-1; M17S1
GI_24497503-A	FOXA2	HNF3B; TCF3B; MGC19807
GI_4557023-S	FOXJ1	HFH4; HFH-4; FKHL13
GI_22024384-S	FPGS	
GI_17738307-S	FREQ	FLUP; NCS1; NCS-1; DKFZp761L1223
GI_27754767-A	FXYD2	HOMG2; ATP1G1; MGC12372
GI_33620741-S	FZR1	FZR; FZR2; HCDH; HCDH1; KIAA1242
GI_20070269-S	G0S2	
GI_11496988-S	GAA	LYAG
GI_9945331-S	GADD45B	MYD118; GADD45BETA; DKFZP566B133
GI_4557616-S	GAS6	AXSF; AXLLG
GI_21361907-S	GBL	
GI_20302161-S	GCG	GLP1; GLP2; GRPP
GI_6382072-S	GCHFR	GFRP; HsT16933
GI_4503970-S	GDI1	GDIL; MRX41; MRX48; OPHN2; XAP-4; RHOGDI; RABGD1A; RABGDIA
GI_28416951-S	GIMAP1	HIMAP1; IMAP38
GI_37540877-S	GLCE	
GI_34147552-S	GLI4	HKR4
GI_31543062-S	GLYCTK	
GI_13435378-S	GMEB2	PIF79; P79PIF; KIAA1269
GI_4504040-S	GNAI2	GIP; GNAI2B
GI_18426899-A	GNAS	AHO; GSA; GSP; POH; GPSA; NESP; GNAS1; PHP1A; PHP1B; GNASXL; NESP55
GI_4885288-S	GNL1	HSR1
GI_4504068-S	GOT2	
GI_13435380-S	GPS1	COPS1
GI_4504106-S	GPX4	snGPx
GI_37552421-S	GRINA	

(continued)

Table S1. (continued)

GI_4504140-S	GRM4	mGlu4; GPRC1D; MGLUR4
GI_4504150-S	GRN	PEPI; PCDGF
GI_4753160-S	GTF3C1	TFIIIC; TFIIIC220; TFIIICalpha
GI_6912587-S	GTPBP6	
GI_34147566-S	GUK1	GMK
GI_33285007-S	GYLTL1B	FLJ35207
GI_38327035-S	HAGH	GL02; GLXII; HAGH1
GI_8923535-S	HCFC1R1	HPIP; FLJ20568
GI_38327036-S	HCN3	KIAA1535
GI_13128861-S	HDAC3	HD3; RPD3; RPD3-2
GI_5729867-S	HERC2	jdf2; p528; D15F37S1; KIAA0393
GI_7705930-S	HERC5	
GI_13128865-S	HEXA	TSD
GI_19923414-S	HEYL	
GI_4504380-S	HGD	AKU; HGO
GI_24496766-S	HGS	HRS; ZFYVE8
GI_5901965-S	HHLA3	
GI_8923568-S	HIF1AN	FIH1; FLJ20615; FLJ22027; DKFZp762F1811
GI_24797066-S	HLA-A	
GI_30581114-A	HM13	H13; SPP; IMP1; PSL3; IMPAS; PSENL3; dJ324017.1
GI_4557644-S	HNRPL	hnRNP-L
GI_4758565-S	HS6ST1	HS6ST
GI_41055988-S	HSMPP8	
GI_13699861-S	HYOU1	ORP150
GI_13027623-S	HYPE	MGC5623; UNQ3041
GI_23503262-S	IBRDC3	
GI_24797154-A	ICMT	PCMT; PPMT; PCCMT; HSTE14; MST098; MSTP098; MGC39955
GI_21361365-S	IFRD2	SM15; IFNRP; SKMc15
GI_6453816-S	IGF2	
GI_10835156-S	IGFBP2	IBP2
GI_10835020-S	IGFBP4	IBP4
GI_24430200-A	IL17RC	IL17-RL; MGC10763
GI_28610153-S	IL8	K60; NAF; GCP1; IL-8; LECT; LUCT; NAP1; 3-10C; CXCL8; GCP-1; LYNAP; MDNCF; MONAP; NAP-1; SCYB8; TSG-1; AMCF-I; b-ENAP
GI_29171685-A	ILKAP	MGC4846; FLJ10181; PP2C-DELTA; DKFZP434J2031
GI_4557670-S	INS	
GI_4557883-S	INSR	
GI_4557672-S	IPF1	IUF1; PDX1; IDX-1; MODY4; PDX-1; STF-1
GI_24308114-S	IRF2BP1	DKFZP434M154
GI_4809285-A	IRF7	IRF7A
GI_21902536-S	ISYNA1	
GI_6006010-A	ITGA3	VL3A; CD49C; GAPB3; MSK18; VCA-2; VLA3a; GAP-B3
GI_21359893-S	ITPK1	ITRPK1
GI_21704285-S	JAM3	FLJ14529
GI_30154219-S	JMJD3	
GI_12056467-A	JUP	DP3; PDGB; PKGB; DPIII
GI_5031816-S	KATNB1	KAT
GI_9506650-S	KCTD5	FLJ20040
GI_7662179-S	KIAA0562	
GI_24308018-S	KIAA0664	
GI_7662439-S	KIAA1001	ARSG
GI_37546881-S	KIAA1414	
GI_21314680-S	KIAA1598	FLJ11122
GI_40548407-I	KIAA1967	DBC1; KIAA1967
GI_13699823-S	KIF11	EG5; HKSP; KNSL1; TRIP5
GI_32307167-S	KIF1A	
GI_19923320-S	KIFC3	
GI_5032176-S	KLF10	EGRA; KLF10; TIEG1
GI_4557700-S	KRT17	PC; K17; PC2; PCHC1
GI_40354194-I	KRT18	K18; CYK18
GI_4504918-S	KRT8	K8; KO; CK8; CYK8; K2C8; CARD2

(continued)

Table S1. (continued)

GI_28212273-S	L3MBTL4	
GI_13569871-S	LBH	DKFZP566J091
GI_38455401-S	LCN2	NGAL
GI_14150030-S	LDOC1L	
GI_23308571-S	LENG4	BB1
GI_6912481-S	LETM1	
GI_6006018-S	LIF	CDF; HILDA; D-FACTOR
GI_4758679-S	LLGL2	HGL
GI_5803022-S	LMAN2	GP36B; VIP36; C50rf8
GI_27436944-A	LMNA	FPL; LFP; EMD2; FPLD; HGPS; LDP1; LMN1; LMNC; PR01; CMD1A; CMT2B1; LGMD1B
GI_37700248-S	LOC253012	
GI_37542183-S	LOC339123	
GI_40786401-S	LOC374395	
GI_31543092-S	LOC89944	
GI_24308395-S	LOC90379	
GI_37541526-S	LOC92154	
GI_12232394-S	LPPR2	FLJ13055
GI_4758685-S	LRP1	APR; LRP; A2MR; CD91; APOER
GI_4505014-S	LRP3	
GI_4758689-S	LRRFIP1	GCF2; TRIP; GCF-2; FLAP-1; HUFI-1; FLIIAP1; MGC10947
GI_7706422-S	LSM7	YNL147W
GI_6996015-A	LTB	p33; TNFC; TNFSF3
GI_31543105-S	LU	AU; BCAM; MSK19
GI_4505048-S	LY6E	RIGE; SCA2; RIG-E; SCA-2; TSA-1
GI_20302149-S	LYPLA2	APT-2; DJ886K2.4
GI_20127485-S	M6PRBP1	
GI_6006019-S	MAD2L2	REV7; MAD2B
GI_9257203-S	MAEA	EMP
GI_31543135-S	MAF1	DKFZp586G1123
GI_14249311-S	MAFG	
GI_9966902-S	MAN1C1	HMIC
GI_10834967-S	MAN2B1	MANB; LAMAN
GI_38202206-S	MAOB	MGC26382
GI_32481208-A	MAPKAPK2	
GI_9845486-A	MARK2	EMK1
GI_13399295-S	MAZ	PUR1; ZF87; SAF-1; SAF-2
GI_5174544-S	MEF2D	
GI_13446228-S	MESDC1	
GI_24308008-S	METAP1	KIAA0094
GI_21362059-S	MGC13114	
GI_20070375-S	MGC15523	
GI_22749382-S	MGC9712	
GI_27486123-S	MICAL3	
GI_20070316-S	MID1IP1	FLJ10386
GI_4505184-S	MIF	GIF; GLIF; MMIF
GI_27436915-A	MINK1	MGC21111
GI_21361271-S	MLLT1	ENL; LTG19
GI_13027797-S	MMP14	MMP-X1; MTMMP1; MT1-MMP
GI_4759109-S	MPDU1	SL15; Lec35
GI_4505232-S	MPG	AAG; MDG; APNG
GI_23510449-S	MPST	MST; TST2; MGC24539
GI_25306271-A	MRPL11	L11mt; CGI-113
GI_27436900-S	MRPL12	5c5-2; L12mt; MRPL7; RPML12; MGC8610; MRPL7/L12; MRP-L31/34
GI_21265079-S	MRPL18	HSPC071; MRP-L18
GI_27436903-S	MRPL23	RPL23; L23MRP; RPL23L
GI_26667176-S	MRPL46	LIECG2; P2ECSL; C150rf4; MGC22762
GI_16950590-A	MRPS12	RPS12; RPMS12; RPSM12; MPR-S12; MT-RPS12
GI_16554600-S	MRPS18A	S18bmt; FLJ10548; MRPS18-3; HumanS18b; MRP-S18-3
GI_16579881-S	MRPS26	GI008; RPMS13; MRP-S13; MRP-S26; NY-BR-87; DJ534B8.3
GI_4505256-S	MSN	
GI_21956644-S	MTPN	V-1; GCDP

(continued)

Table S1. (continued)

GI_37541581-S	MUC5B	
GI_34147593-S	MUS81	FLJ21012
GI_31377612-S	MYADM	
GI_7657350-S	MYBBP1A	P160; PAP2
GI_33563339-S	MYH14	NHMCII; FLJ13881; KIAA2034
GI_24415399-S	MY01C	myr2; MY01E
GI_4505328-S	NAPA	SNAPA; ALPHASNAP; alpha SNAP
GI_14042973-S	NCALD	
GI_19923386-S	NCBP2	NIP1; CBP20
GI_24638432-S	NCSTN	APH2; KIAA0253
GI_10800414-S	NDN	HsT16328
GI_28269680-S	NDUFA11	B14.7
GI_33519471-S	NDUFB7	B18; CI-B18; MGC2480
GI_13375816-S	NEIL1	NEI1; hFPG1; FLJ22402
GI_19923222-S	NFKB2	LYT10; LYT-10
GI_26787990-S	NFKBIL1	IKBL; NFKBIL
GI_11496977-S	NFYC	HSM; CBFC; HAP5; CBF-C; NF-YC; H1TF2A
GI_4505394-S	NID	NID1; ENTACTIN
GI_31543289-S	NINJ1	NIN1; NINJURIN
GI_32307133-S	NKX2-2	NKX2B; NKX2.2
GI_41204930-S	NLF2	
GI_37693992-S	NME3	DR-nm23
GI_34147607-S	NOSIP	CGI-25
GI_20149616-S	NPDC1	CAB; CAB-; CAB1; CAB-1; DKFZP586J0523
GI_13430847-S	NR1D1	EAR1; hRev; THRA1; THRAL; ear-1
GI_21070966-A	NRXN1	Hs.22998; KIAA0578
GI_21070970-A	NRXN3	KIAA0743
GI_38455392-S	NTHL1	NTH1; OCTS3
GI_20070227-S	NUCB1	NUC
GI_34486089-S	OAZ1	OAZ
GI_8922715-S	OGDHL	
GI_33286445-S	OGFR	
GI_8923113-S	OTUB1	
GI_20070124-S	P4HB	DSI; GIT; PDI; P04DB; P04HB; PROHB; ERBA2L
GI_7382497-S	PAK4	
GI_21536446-S	PAK6	PAK5
GI_16418340-S	PANX2	hPANX2
GI_23097271-S	PAOX	PAO; DKFZp434J245
GI_8394416-S	PARD6A	PAR-6; TAX40; PAR-6A; TIP-40; PAR6alpha
GI_20127527-S	PARVB	CGI-56; BK414D7.C22.1.MRNA
GI_14670372-A	PCBP4	LIP4; MCG10
GI_42659678-S	PCNXL3	
GI_4505650-S	PCYT2	ET
GI_4505694-S	PDPK1	PDK1; PR00461
GI_30061508-A	PDZK3	AIPC; PIN1; PAPIN; PDZD2; KIAA0300
GI_24415382-S	PELP1	MNAR; P160
GI_22538479-A	PEMT	PNMT; PEAMT; PEMPT; PEMT2; MGC2483
GI_28372500-S	PERLD1	PP1498; AGLA546; MGC9753
GI_22507392-S	PERQ1	GIGYF1; AF053356-CDS2
GI_22091458-S	PES1	PES
GI_24797087-A	PEX10	NALD; RNF69; MGC1998
GI_4758899-S	PFKFB3	IPFK2
GI_19923257-S	PFKFB4	
GI_16753216-A	PFN2	PFL; D3S1319E
GI_21359898-S	PGEA1	CBY; arb1; HS508I15A
GI_6912585-S	PGLS	6PGL
GI_8923197-S	PGPEP1	PGP; Pcp; PGPI; PGP-I; FLJ20208
GI_37595529-A	PHC2	EDR2; HPH2
GI_24475860-S	PHPT1	CGI-202; HSPC141; DKFZp564M173
GI_24850132-S	PIAS4	MGC35296
GI_22538452-A	PIGQ	GPI1; hGPI1; MGC12693

(continued)

Table S1. (continued)

GI_23397652-S	PIGT	CGI-06; MGC8909
GI_4505808-S	PIK4CB	PI4Kbeta; PI4K-BETA
GI_30179910-A	PILRB	FDFACT1; FDFACT2
GI_32483384-A	PKIG	
GI_4506072-S	PKN1	DBK; PKN; PRK1
GI_11386138-S	PLCB3	
GI_41322918-I	PLEC1	PCN; EBS1; EBSO; PLTN
GI_20070288-S	PLEKHA3	FAPP1; FLJ20067
GI_29789005-S	PLEKHC1	MIG2; KIND2; mig-2; UNC112
GI_8922332-S	PLEKHJ1	
GI_34147645-S	PLOD3	LH3
GI_31543416-S	PLSCR3	
GI_8923792-S	PLXNA3	HSSEXGENE
GI_6005831-S	PMF1	
GI_5453923-S	POLD2	
GI_30089946-S	POLDIP2	
GI_14589950-S	POLR2E	RPB5; XAP4; RPABC1; hRPB25; hsRPB5
GI_14589956-S	POLR2L	RPB10; RPABC5; RPB7.6; hRPB7.6; hsRPB10b; RPB10beta
GI_42560241-I	POU5F1	OCT3; OTF3; OTF4; Oct4; MGC22487
GI_31543427-S	PPAN	SSF1; MGC14226; MGC45852
GI_29826283-A	PPM1G	PP2CG; PPP2CG; MGC1675; MGC2870; PP2CGAMMA
GI_9790902-S	PPP1R15A	GADD34
GI_4506026-S	PPP4C	PP4; PPX
GI_20127496-S	PPP5C	PP5; PPP5
GI_7110696-S	PRKCABP	PICK1; dJ1039K5
GI_35493938-S	ProSAPiP1	KIAA0552
GI_22538484-S	PRPSAP2	PAP41
GI_21071012-S	PRSS2	TRY2; TRY8; TRYP2
GI_21614535-S	PRSS22	BSSP-4; MGC9599; SP001LA; hBSSP-4
GI_6912705-S	PSD4	EFA6B
GI_7108359-A	PSEN2	AD4; PS2; AD3L; STM2
GI_24430154-A	PSMC4	S6; TBP7; MIP224; MGC8570; MGC13687; MGC23214
GI_25777599-S	PSMD1	S1; P112
GI_28605136-A	PSMD10	p28
GI_25777611-S	PSMD3	S3; P58; RPN3
GI_34147588-S	PTGES2	GBF1; PGES2; C90rf15; FLJ14038; MGC11289
GI_27886606-A	PTK7	CCK4
GI_34594666-S	PTMS	
GI_14589853-A	PTP4A3	PRL3; PRL-3; PRL-R
GI_18860905-S	PTPRN	IA2; IA-2; ICA512; R-PTP-N; IA-2/PTP
GI_19743920-A	PTPRS	PTPSIGMA
GI_19743928-A	PTPRT	RPTPrho; KIAA0283
GI_19743932-A	PTPRU	FMI; PTP; PCP-2; PTP-J; PTPRO; PTPU2; GLEPP1; PTP-PI; PTPPSI; hPTP-J; R-PTP-PSI
GI_34147590-S	PUS1	
GI_23503258-S	PUSL1	
GI_28195387-S	RAB11FIP4	KIAA1821; MGC11316
GI_42734506-S	RAB26	V46133
GI_37550536-S	RAB43	
GI_21361508-S	RAB4B	
GI_13376207-S	RABEP2	FLJ23282
GI_33469950-A	RABGGTA	
GI_23111014-I	RAI1	SMS; SMCR; KIAA1820; MGC12824; DKFZP434A139
GI_24307908-S	RALGDS	RGF; RalGEF
GI_40538735-S	RANBP10	KIAA1464
GI_19718756-S	RANBP2	NUP358
GI_38201688-S	RANGAP1	Fug1; KIAA1835; MGC20266
GI_4506418-S	RARA	RAR; NR1B1
GI_22027484-S	RASD1	AGS1; DEXRAS1; MGC:26290
GI_37545358-S	RASL11A	
GI_33457331-S	RAVER1	KIAA1978
GI_30181230-S	REG1B	REGH; REGL; PSPS2; REGI-BETA

(continued)

Table S1. (continued)

GI_35493877-S	RELB	I-REL
GI_18375672-S	RENT1	UPF1; HUPF1; NORF1; pNORF1; KIAA0221
GI_19923392-S	RERE	ARG; ARP; DNB1; ATN1L; KIAA0458
GI_34147664-S	RGS14	
GI_5031704-S	RGS19	GAIP; RGSGAIP
GI_10835048-S	RHOA	RHOA; ARH12; RH012; RHOH12
GI_4502218-S	RHOG	
GI_35493905-S	RIN2	RASSF4
GI_34878786-S	RNF25	A07; FLJ13906
GI_37588854-A	RNF40	BRE1B; RBP95; STARING; KIAA0661; MGC13051
GI_20070295-S	RNPEPL1	FLJ10806
GI_17981705-S	RPS4X	CCG2; SCAR; SCR10; DXS306
GI_4506738-S	RPS6KB2	p70S6Kb; P70-BETA
GI_4759053-S	RRAD	RAD; RAD1; REM3
GI_10863934-S	RTN1	NSP
GI_21264342-S	SAFB	HAP; HET; SAFB1
GI_37574611-S	SBF1	MTMR5
GI_16445417-S	SCAMP2	
GI_33598936-A	SCARF2	SREC2; SREC-II; SRECRP-1
GI_39930609-I	SCN1B	GEFSP1
GI_21703709-S	SCOTIN	
GI_33186909-A	SCRIB	CRIB1; SCRB1; SCRIB1; Vartul; KIAA0147
GI_14150018-S	SCRT1	
GI_8922466-S	SDAD1	
GI_5032082-S	SDCBP	ST1; SYCL; MDA-9; TACIP18; SYNTENIN
GI_38016915-A	SDCBP2	ST-2; SITAC18
GI_11545742-S	SDF2L1	
GI_38202213-S	SEC23A	MGC26267
GI_14591931-S	SEC61A1	HSEC61
GI_24308274-S	SELB	EFSEC; EEFSEC
GI_17975596-S	SELM	
GI_39777609-I	SEMA4B	SemC; SEMAC; KIAA1745
GI_24234731-A	SEMA6D	FLJ11598; KIAA1479
GI_4506886-S	SEPW1	selW
GI_21361197-S	SERPINA1	PI; A1A; AAT; PI1; A1AT; alpha-1-antitrypsin
GI_9665246-S	SERPINA3	ACT; AACT
GI_21361301-S	SERPINA4	KAL; KST; PI4; KLST; kallistatin
GI_4505148-S	SERPINB7	MEGSIN
GI_7019524-S	SERTAD1	
GI_32189413-S	SF3A2	PRP11; SAP62; SF3a66
GI_33469963-A	SF4	RBP; F23858; DKFZp434E2216
GI_37563661-S	SFI1	
GI_8400734-S	SFRP5	SARP3
GI_21389350-S	SFXN5	BBG-TCC
GI_31543619-S	SGSH	HSS; SFMD; MPS3A
GI_21361603-S	SH3TC1	
GI_31542518-S	Sharpin	
GI_28373091-A	SIAT7D	SIAT3C; ST6GALNAC4; ST6GALNACIV
GI_11141876-S	SIGIRR	
GI_31543622-S	SIL1	BAP
GI_24497626-A	SIPA1	SPA1; MGC17037
GI_13775601-A	SIRT2	SIR2L; SIR2L2
GI_34147624-S	SIX2	
GI_19913344-S	SLBP	HBP
GI_5730042-S	SLC12A7	KCC4; DKFZP434F076
GI_20127461-S	SLC16A5	MCT5
GI_21389314-S	SLC25A1	CTP; SLC20A3
GI_10835018-S	SLC29A2	ENT2; DER12; HNP36
GI_27777666-S	SLC30A8	ZnT-8
GI_22748628-S	SLC39A13	FLJ25785

(continued)

Table S1. (continued)

GI_27734776-S	SLC39A5	
GI_23308570-S	SLC3A1	D2H; ATR1; NBAT; RBAT; CSNU1
GI_34147653-S	SLC3A2	4F2; CD98; MDU1; 4F2HC; NACAE
GI_21361550-S	SLC4A2	AE2; HKB3; BND3L; NBND3; EPB3L1
GI_5032096-S	SLC6A8	CT1; CRTR
GI_34222350-S	SLC7A5	E16; CD98; LAT1; MPE16; D16S469E
GI_5454069-S	SLC9A6	NHE6; KIAA0267
GI_21071055-S	SMARCA4	BRG1; BAF190; SNF2L4; SNF2LB; hSNF2B; SNF2-BETA
GI_27545325-S	SMARCB1	RDT; INI1; SNF5; Snr1; BAF47; Sfh1p; hSNFS; SNF5L1
GI_21237807-A	SMARCC2	Rsc8; BAF170; CRACC2
GI_21264350-S	SMARCD2	BAF60B; CRACD2; PR02451
GI_34147321-S	SMPDL3A	
GI_12232400-S	SMYD3	ZMYND1; ZNFN3A1; FLJ21080
GI_31543647-S	SNRP70	RPU1; U1AP; U170K; U1RNP; RNPU1Z
GI_4507150-S	SOD3	
GI_41282001-I	SPHK1	SPHK
GI_4507178-S	SPINK1	PCTT; PSTI; TATI
GI_41281781-I	SPPL2B	IMP4; PSL1; KIAA1532
GI_22507315-S	SPTB	
GI_32698749-S	SR-A1	
GI_27477112-S	SREBF2	SREBP2
GI_22507413-S	SRMS	SRM; C200rf148; dJ697K14.1
GI_24497619-S	SRP68	
GI_21314683-A	SSBP3	SSDP; SSDP1; SSDP3; FLJ10355
GI_14249149-S	SSBP4	MGC3181
GI_4505324-S	SSNA1	N14; NA14
GI_5453837-S	SSSCA1	p27
GI_4507242-S	SST	SMST
GI_8923213-S	STAP2	BKS; STAP-2; FLJ20234
GI_23397677-S	STAT6	STAT6B; STAT6C; D12S1644; IL-4-STAT
GI_4507266-S	STC2	STC-2; STCRP
GI_5454093-S	STK3	KRS1; MST2
GI_7019572-S	STRN4	ZIN; zinedin
GI_4507284-S	STX10	SYN10; hsyn10
GI_4759181-S	STX1A	STX1; HPC-1; p35-1
GI_34147519-S	STX6	
GI_5902127-S	STXBP2	UNC18B; UNC18-2; MUNC18-2
GI_6005885-S	STXBP3	PSP; MUNC18C; UNC-18C; MUNC18-3
GI_19557701-S	SURF6	FLJ30322
GI_32401419-S	SYNPR	SPO; MGC26651
GI_31342626-S	SYT12	SRG1; SYT11
GI_38194226-S	SYT7	SYT-VII
GI_21536354-A	TAF6	TAF2E; TAFII70; TAFII80; TAFII85; MGC:8964
GI_11993942-S	TAX1BP3	
GI_24308016-S	TBC1D1	TBC; TBC1; KIAA1108
GI_8400735-S	TBCD	KIAA0988
GI_34222210-S	TCBA1	MGC41924
GI_19924146-A	TCIRG1	a3; Stv1; Vph1; Atp6i; OC116; OPTB1; TIRC7; ATP6N1C; ATP6V0A3; OC-116kDa
GI_20127439-S	TETRAN	TETTRAN
GI_34147580-S	TEX264	SIG11
GI_21359903-S	TFE3	RCCP2
GI_24307932-S	TFEB	TCFEB
GI_7019370-S	TFPT	FB1; amida
GI_33589847-S	TFR2	HFE3
GI_17572809-S	THOC4	ALY; BEF
GI_34222291-S	THOP1	
GI_7661929-S	THRAP4	
GI_5032180-S	TIMM17B	JM3; TIM17B; DXS9822
GI_4507508-S	TIMP1	EPA; EPO; HCI; CLGI; TIMP
GI_33636700-S	TK2	
GI_21265109-S	TM4SF4	ILTMP; il-TMP; FLJ31015

(continued)

Table S1. (continued)

GI_4507546-S	TM7SF2	ANG1
GI_8922460-S	TMEM38B	
GI_42657651-S	TMEM63B	
GI_13994299-S	TMPIT	
GI_4507554-S	TMPO	TP; LAP2
GI_7706185-S	TNFRSF12A	FN14; TWEAKR
GI_23200040-S	TNFRSF14	TR2; ATAR; HVEA; HVEM; LIGHTR
GI_23238201-A	TNFRSF19	TAJ; TROY; TRADE; TAJ-alpha
GI_23312372-S	TNFRSF1A	FPF; p55; p60; TBP1; TNF-R; TNFAR; TNFR1; p55-R; CD120a; TNFR55; TNFR60; TNF-R-I; TNF-R55; MGC19588
GI_21361267-S	TNIP1	VAN; NAF1; ABIN-1; KIAA0113
GI_7657256-S	TOMM20	
GI_4557540-S	TOR1A	DQ2; TOR1A
GI_18497297-S	TOR2A	TORP1; FLJ14771
GI_4507652-S	TPMT	
GI_14150010-S	TRAF7	TRAF7; RNF119; DKFZp586I021
GI_10864020-S	TRAPPC1	BET5; MUM2
GI_31542264-S	TRIB3	NIPK; SINK; TRB3; SKIP3; TRIB3
GI_41281980-I	TRIF	TICAM1; PRVTIRB; MGC35334
GI_24497621-S	TRIM11	BIA1; RNF92
GI_14971416-S	TRIM28	KAP1; TF1B; RNF96; TIF1B
GI_16445353-A	TRIM31	RNF; HCG1; HCGI; C60rf13
GI_11342675-S	TRIP10	CIP4
GI_31542640-S	TRMT1	
GI_18158415-S	TRPC4AP	TRUSS; TRRP4AP; C200rf188
GI_34303921-S	TRUB1	
GI_21071005-S	TSSC4	
GI_34335291-S	TST	RDS; MGC19578
GI_17921988-S	TUBA1	FLJ30169; H2-ALPHA
GI_5729839-S	TUBGCP2	GCP2; Spc97p
GI_21361510-S	TXNDC11	
GI_18104958-S	TXNDC9	
GI_5454143-S	UBD	FAT10
GI_32967281-S	UBE2B	HR6B; UBC2; HHR6B; RAD6B; E2-17kDa
GI_33359690-A	UBE2E1	UBCH6
GI_37577133-S	UBE2M	UBC12; hUbc12; UBC-RS2
GI_7657045-S	UBE2S	
GI_34222339-S	UBTD1	
GI_7657670-S	UBTF	UBF; NOR-90
GI_13376853-S	UBXD1	UBXDC2
GI_16596691-S	UCN3	SCP; SPC; UCNIII
GI_4507818-S	UGT2B15	UGT2B8
GI_23199984-S	ULK2	KIAA0623
GI_4507846-S	USF2	FIP
GI_22550103-S	USP32	USP10; NY-REN-60
GI_10863942-S	UTX	
GI_4507868-S	VASP	
GI_18379348-S	VAT1	VATI; FLJ20230
GI_7669552-S	VCP	p97; TERA
GI_4507894-S	VIM	
GI_42544225-S	VPS18	KIAA1475
GI_37674208-S	WDR18	MGC2436; R32184_1
GI_31317275-A	WDR20	DMR; FLJ33659; MGC33177; MGC33183
GI_31657100-A	WDR23	GL014; PR02389
GI_34147468-S	WDR34	
GI_11072092-I	WDR6	FLJ10218
GI_22095348-S	WDTC1	
GI_13376995-S	WFS1	WFS; WFRS; DFNA6; DFNA14; DFNA38; DIDMOAD; WOLFRAMIN
GI_19913362-S	WHSC2	NELFA; FLJ10442; FLJ25112; P/OKc1.15
GI_17402921-S	WNT4	WNT-4

(continued)

Table S1. (continued)

GI_8051634-S	XP01	CRM1
GI_19923271-S	XPR1	X3; SYG1
GI_4507996-S	ZBTB17	MIZ1; pHZ-67
GI_15812177-S	ZFP36L2	BRF2; ERF2; ERF-2; TIS11D
GI_31563371-A	ZGPAT	FLJ14972; MGC44880; dJ583P15.3
GI_6005965-S	ZNF146	OZF
GI_31543982-S	ZNF289	IRZ; Zfp289; FLJ14576
GI_37622344-A	ZNF42	MZF1; MZF-1; MZF1B
GI_24432061-S	ZNF513	
GI_23397478-S	ZNF524	
GI_21687263-S	ZNF558	
GI_27734902-S	ZNF584	
GI_4508034-S	ZNF7	KOX4; HF.16
GI_18599776-S	ZYG11B	
GI_38202225-S	ZZEF1	
GI_5032100-S	ABCC5	MRP5; SMRP; ABC33; MOATC; MOAT-C; pABC11; EST277145
GI_11545766-S	ABHD4	FLJ12816
GI_21327681-S	ACADM	MCAD; ACAD1; MCADH
GI_4557232-S	ACADS	SCAD; ACAD3
GI_7710156-A	ACHE	YT
GI_13325060-S	ACTR1B	ARP1B; CTRN2

transgene, and the red channel to assess autofluorescence. DAPI fluorescence produced a nuclear mask that allowed the microscope to focus from well to well on the plate.

Image processing (Cytoshop, Beckman Coulter) was used to perform shade correction, nuclear segmentation, and cytometry. Due to lamp variations throughout the imaging process, shade correction and plate-to-plate normalization techniques were used by equilibrating plate and global medians. Cell-by-cell analysis was performed by tessellation and pixel intensity measurements. The segmentation protocol involved the following steps:

1. The nucleus of each cell was identified using Cytoshop's nuclear segmentation algorithm that included an "open" morphological operation.
2. Equidistance tessellation lines were drawn between the centroids of the identified nuclei, effectively breaking up the images into cellular regions.
3. An Object Extraction Correlation radius of 30 pixels was set, inside which pixels were assumed to belong to the cytoplasm of the cell.

Hits were then determined by applying threshold intensity gates on the green channel and surveying the number of cells above or below that gate in a given well by analyzing the average green pixel intensity under the cytoplasmic mask. These counts were then normalized to the total number of cells per well to give a percent GFP-positive cells quotient. To construct the final assay-wide database from the individual plate databases, we used a MATLAB algorithm to collate the individual plate data.

Chronic ethopropazine treatment

T6PNE cells were seeded in a 10-cm dish with 0.5 µM tamoxifen. At 24 h, either 15 µM ethopropazine or a vehicle control was added. At 96 h, the cells were passed into either a 384-well clear-bottom black well plate for imaging or a 10-cm dish for continued culture along with fresh ethopropazine or vehicle. The same passing procedure was performed every 3 days for the remainder of the 12-day experiment. The 384-well plates seeded for imaging were fixed in 4% formaldehyde 24 h after they were seeded. DAPI was then added at a final concentration of 167 µg/mL. The plates were imaged on the IC 100 in the blue and green channels, and Cytoshop analysis was then performed to determine the percentage of cells in each well that contained GFP above a threshold determined by a MATLAB algorithm (% GFP+). Fold change in % GFP+ cells per well treated with ethopropazine (15 µM) versus vehicle control was measured over 12 days ($n = 3$; error bars are standard error; $p < 0.05$).

Phenothiazine structure-activity relationship

T6PNE cells were seeded at 1750 cells per well in clear-bottom black 384-well plates with 0.5 µM tamoxifen. At 24 h, the phenothiazine or vehicle was added at a concentration range of 1.25 to 20 µM. Cells were fixed with 4% formaldehyde at 72 h. DAPI was then added at a final concentration of 0.167 µg/mL. The

plates were imaged on the IC 100 in the blue and green channels, and Cytoshop analysis was then performed to determine the percentage of cells in each well that contained GFP above a threshold determined by a MATLAB algorithm (% GFP+).

REFERENCES

1. Itkin-Ansari P, Marcora E, Geron I, Tyrberg B, Demeterco C, Hao E, et al: NeuroD1 in the endocrine pancreas: localization and dual function as an activator and repressor. *Dev Dyn* 2005;233:946-953.
2. Halvorsen TL, Beattie GM, Lopez AD, Hayek A, Levine F: Accelerated telomere shortening and senescence in human pancreatic islet cells stimulated to divide in vitro. *J Endocrinol* 2000;166:103-109.
3. Engel I, Murre C: Ectopic expression of E47 or E12 promotes the death of E2A-deficient lymphomas. *Proc Natl Acad Sci USA* 1999;96:996-1001.
4. Alheim K, Corness J, Samuelsson MK, Bladh LG, Murata T, Nilsson T, et al: Identification of a functional glucocorticoid response element in the promoter of the cyclin-dependent kinase inhibitor p57Kip2. *J Mol Endocrinol* 2003;30:359-368.
5. Weintraub H, Davis R, Lockshon D, Lassar A: MyoD binds cooperatively to two sites in a target enhancer sequence: occupancy of two sites is required for activation. *Proc Natl Acad Sci USA* 1990;87:5623-5627.
6. Carlesso N, Aster JC, Sklar J, Scadden DT: Notch1-induced delay of human hematopoietic progenitor cell differentiation is associated with altered cell cycle kinetics. *Blood* 1999;93:838-848.
7. Hao E, Tyrberg B, Itkin-Ansari P, Lakey JR, Geron I, Monosov EZ, et al: Beta-cell differentiation from nonendocrine epithelial cells of the adult human pancreas. *Nat Med* 2006;12:310-316.
8. Singer O, Marr RA, Rockenstein E, Crews L, Coufal NG, Gage FH, et al: Targeting BACE1 with siRNAs ameliorates Alzheimer disease neuropathology in a transgenic model. *Nat Neurosci* 2005;8:1343-1349.
9. Tiscornia G, Singer O, Ikawa M, Verma IM: A general method for gene knockdown in mice by using lentiviral vectors expressing small interfering RNA. *Proc Natl Acad Sci USA* 2003;100:1844-1848.
10. Ball AJ, Abrahamsson AE, Tyrberg B, Itkin-Ansari P, Levine F: HES6 reverses nuclear reprogramming of insulin-producing cells following cell fusion. *Biochem Biophys Res Commun* 2007;355:331-337.